Comparison of total water vapour content in the Arctic derived from GNSS, AIRS, MODIS and SCIAMACHY

Dunya. Alraddawi[1], Alain. Sarkissian[1], Philippe. Keckhut[1], Olivier. Bock[2], Stefan. Noël[3], Slimane. Bekki[1], Abdenour. Irbah[1], Mustapha. Meftah[1], Chantal. Claud[1,4]

[1]OVSQ-LATMOS, University Paris Saclay, Guyancourt 78280, France
[2]IGN-LAREG, University Paris Diderot, Paris 75013, France
[3]Institute of Environmental Physics, University of Bremen, 28334 Bremen, Germany
[4]LMD/IPSL, CNRS, École Polytechnique, Université Paris Saclay, ENS, PSL Research University, Sorbonne Universités, UPMC Univ Paris 06, Palaiseau, France

Corresponding author: Alain Sarkissian (alain.sarkissian@latmos.ipsl.fr)

Abstract. Atmospheric water vapour plays a key role in the Arctic radiation budget, hydrological cycle and hence climate, but its measurement with high accuracy remains an important challenge. Total Column Water Vapour (TCWV) data set derived from ground-based GNSS measurements are used to assess the quality of different existing satellite TCWV datasets, namely from the Moderate Resolution Imaging Spectrometer (MODIS), the Atmospheric Infrared System (AIRS), and the SCanning Imaging Absorption spectroMeter for Atmospheric CHartographY (SCIAMACHY). The comparisons between GNSS and satellite data are carried out for three reference Arctic observation sites (Sodankyla, Ny-Alesund and Thule) where long homogeneous GNSS time series of more than a decade (2001-2014) are available. We select hourly GNSS data that are coincident with overpasses of the different satellites over the 3 sites and then average them into monthly means that are compared with monthly mean satellite products for different seasons. The agreement between GNSS and satellite time series is generally within 5% at all sites for most conditions. The weakest correlations are found during summer. Among all the satellite data, AIRS shows the best agreement with GNSS time series, though AIRS TCWV is often slightly too high in drier atmospheres (i.e. high latitude stations during fall and winter). SCIAMACHY TCWV data are generally drier than GNSS measurements at all the stations during the summer. This study suggests that these biases are associated with cloud cover, especially at Ny-Alesund and Thule. The dry biases of MODIS and SCIAMACHY observations are most pronounced at Sodankyla during the snow season (from October to March). Regarding SCIAMACHY, this bias is possibly linked to the fact that the SCIAMACHY TCWV retrieval does not take accurately into account the variations in surface albedo, notably in the presence of snow with a nearby canopy as in Sodankyla. The MODIS bias at Sodankyla is found to be correlated with cloud cover fraction and is also expected to be affected by other atmospheric or surface albedo changes linked for instance to the presence of forests or anthropogenic emissions. Overall, the results point out that a better estimation of seasonally-dependent surface albedo and a better consideration of vertically-resolved cloud cover are recommended if biases in satellite measurements are to be reduced in polar regions.

1 Introduction

Water vapour has an important role in the Earth radiative balance (e.g. *Kiehl and Trenberth, 1997; Trenberth and Stepaniak, 2003; Ruckstuhl et al., 2007; Trenberth et al., 2007)*, hydrologic cycle (e.g. Chahine, 1992; Serreze *et al.*, 2006; Jones *et al.*, 2007; Hanesiak *et al.*, 2010); and climat change (e.g. *Schneider et al., 1999, 2010; Held and Soden, 2000; Ramanathan and Inamdar, 2006; Rangwala et al., 2009)*. The rate of the Arctic climate change is twice larger than the global one due to greenhouse gases (GHG) increase. The water vapour feedback loop is highlighted, as part of many others, responsible of the Arctic amplification (e.g. *Winton, 2006; Francis and Hunter, 2007; Miller et al., 2007; Screen and Simmonds, 2010; Chen et al., 2011; Ghatak and Miller, 2013)*.

Water vapour measurements (total column / vertical profile information) are available using radiosondes since early 1940s and satellites since 1980s primarily for meteorological purposes, while GPS (Global Positioning System) has been used more recently (1990s) for humidity observations (Bevis et al., 1992b) .

The Total Column of Water Vapour (TCWV), also called Integrated Water Vapour (IWV), is defined as the density of water vapour in an atmospheric column over a unit area (kg m^{-2}). It is also sometimes referred as Precipitable Water (PW), which represents the height of liquid water (in mm) resulting from the condensation of all the water vapour of a vertical column over a unit area.

TCWV is characterized by large spatial and temporal variability. It affects the water cycle intensity and the atmospheric dynamics *(Sherwood et al., 2010; Trenberth et al., 2005)*. Since 2010, the Global Climate Observing System (GCOS) declared the TCWV as an essential climate variable, and highlighted the importance of high resolution long time series that could enable the detection of both local and global TCWV trends.

The available satellite remote sensing techniques to observe TCWV in Micro Wave (MW), Infra Red (IR), Near Infra Red (NIR), and VISible (VIS) spectral domains are promising, with a global coverage that enables climate studies, but with limited retrieval capability (e.g. only day time, only clear skies, or over oceans only). Satellite observations are validated by ground-based techniques, traditionally radiosondes. However, radiosonde data suffer sometimes from systematic observational errors, and spatial and temporal inhomogeneity and instability *(Gaffen, 1994; Wang, 2003),* that could induce potentially regional biases, if radiosondes alone are used to validate satellite data (*Wang and Zhang, 2008, 2009; Bock and Nuret, 2009)*

GPS measurements emulate global radiosonde data as another confident reference to validate satellites and regional models (e.g. *Bock et al., 2007*, and references therein). GPS TCWV measurements are independent of the weather, performed with high temporal resolutions (a few minutes), and have continuously improved resolution (a few km for some local networks). While GPS is based on a delay measurement, it can be applied similarly to different sensors, and is an ideal tool for long-term measurements, despite it can experience bias in certain specific configurations.

Currently, satellite derived water vapour accuracy is still not very well- known compared to GPS, especially over cold regions. Few previous studies approached this topic, most of which used different versions of GPS GNSS data. For example, *(Thomas et al., 2011)* compared GPS to MODIS and AIRS over 13 Antarctic stations for 2004, and found that GPS TCWV data are drier than MODIS, while wetter than AIRS. *(Palm et al., 2010)* compared GPS with SCIAMACHY and GOME-2A data over Ny-Alesund/Arctic, GPS under-estimated both satellites sensors.

The current study provides inter-comparisons of various measurements and methods allowing to quantify uncertainties, accuracies, and limits of several global sensors/techniques available which in turn helps improving the data analysis methods *(Bock, 2012; Guerova et al., 2005, 2016)* and potential trend estimates.

In this publication, we use a recently reprocessed version of GNSS TCWV (combined GPS and GLONASS) data with hourly temporal sampling covering the period from 1996 to 2014. It enabled the largest number of coincident overpasses of three independent selected satellites AIRS/IR (from 2003 to 2014), MODIS/NIR (from 2001 to 2014), and SCIAMACHY/VIS (from 2003 to 2011) for inter-comparisons. Three Arctic ground-based observation sites were chosen where GNSS data are processed for TCWV observations, namely: Ny-Alesund (78°N, 12°E), Thule (76°N, 69°W), and Sodankyla (67°N, 26°E). Satellite gridded data were matched with these stations within a maximum spatial distance of 50 km.

The global validation efforts of the used satellites products discussed many factors affecting the satellites biases. For example, both MODIS *(Gao and Kaufman, 2003)* and AIRS *(Fetzer et al., 2006)* TCWV retrievals are limited by the accurate initialization of the humidity profile. While SCIAMACHY measurements are independant of initial humidity profile, but affected by other factors like the albedo estimation for different surfaces *(Noël, 2007),* MODIS measurements are known to be affected by hazy conditions, and to be less accurate over dark surfaces (albedo effect like SCIAMACHY). Generally, satellites measurements are more accurate during clear sky conditions. However cloud clearing is a challenging task. The present publication uses cloud cleared products in order to assess their uncertainties for three Arctic stations. Moreover, it investigates the possible relation between these three satellites biases and the cloud cover making use of an available cloud fraction product to facilitate the study.

Section 2 describes the datasets used. Section 3 presents results of TCWV comparisons. Section 4 discusses the results suggesting the link between observed biases in the satellite data and cloud cover which is shown to be a limiting factor in the retrieval of visible, near-infrared and infrared TCWV data from space. Section 5 presents conclusions.

2 Description of the data sets

2.1 GNSS

Originally designed for real-time navigation and positioning, GNSS was rapidly seen as a cheap and accurate technique for measuring TCWV from the ground *(Bevis et al., 1992a)*. The principle consists in estimating the propagation delay induced by the atmosphere of the microwave signals emitted by the GNSS satellites and received by ground-based receivers. The Zenith Tropospheric Delay (ZTD) is usually parsed into its wet and hydrostatic components (ZWD and ZHD, respectively for Zenith Wet Delay, and Zenith Hydrostatic Delay). Accurate estimations of surface pressure and a weighted mean temperature are required to convert GNSS ZTD into TCWV using the following formulas *(Bevis et al., 1992b)*

$$\mathrm{ZWD} = \mathrm{ZTD} - \mathrm{ZHD}, \qquad (1)$$

where ZTD is the GNSS ZTD estimate, ZHD is computed from the surface pressure *(Davis et al., 1985)*:

$$ZHD = 0.002277\ P_{sfc} / f(\lambda, H),$$

Where P_{sfc} is the surface pressure, λ and H are the latitude and altitude of the station, $f(\lambda, H)$ accounts for the ˇ geographical variation of the mean acceleration due to gravity *(Davis et al., 1985)*.

TCWV is converted from the ZWD as:

$$TCWV = ZWD * K(T_m), \qquad (2)$$

Where $K(T_m)$ is a delay to mass conversion factor and T_m is the weighted mean temperature.

In this study, we used GNSS ZTD data from the Geodetic Observatory Pecny (Czech Republic) named “repro2 solution” and referred to as GO4 *(Dousa et al., 2017)*. This GNSS solution was produced with a homogeneous and optimized processing strategy. Outliers in the ZTD time series were detected and removed using the range-check and outlier check method described in *(Bock et al., 2014)*. ZHD and T_m were computed from the ERA-Interim reanalysis pressure level data (37 vertical levels between 1000 hPa and 1 hPa, 0.75° x 0.75° horizontal resolution, 6-hourly time resolution) (*Dee et al., 2011)*. The data were first interpolated vertically to the height of the GNSS station and then interpolated horizontally (bi-linear interpolation using the 4 grid-points surrounding the station) to the location of the station. The 6-hourly P_{sfc} and T_m data were then interpolated (with cubic splines) to the times of the GNSS ZTD data resulting in the final 1-hourly GNSS TCWV dataset.

In order to overcome the satellite/GNSS timing error due to limited hours of MODIS/AIRS/SCIAMACHY measurements during a month over a fixed point at the surface, the satellites passing hours over the three Arctic GNSS stations were defined through the IXION software (http://climserv.ipsl.polytechnique.fr/ixion/index.php). For each satellite, only GNSS TCWV corresponding to the over-passes less than 1 hour (Table 1) were used to calculate the corresponding monthly time series.

Seasonal variations of the TCWV over all three sites for a common period of 11 years (2004-2014) exhibit a pronounced seasonal cycle (Fig. 1) with mean values ranging from a maximum in July of 20, 14, 13 kg m^{-2}, to a minimum in winter of 6, 4.5, 2 kg m^{-2} over Sodankyla, Ny-Alesund and Thule respectively.

Extreme hourly values could reach 40 kg m^{-2} (not shown) over Sodankyla. This highest amplitude appears in summer under continental climate conditions. Ny-Alesund and Thule have likely similar seasonal features. However, Thule has drier winter/fall periods due to the Greenland ice sheet climate effect. “Figure 2 shows that the year to year variations of TCWV at the three stations are smaller than the seasonal cycle (Fig.1). This can be easily seen for summer values (peak values).”

2.2 MODIS

The passive imaging spectral radiometer is installed on both platforms (Terra and Aqua) of the Earth Observing System (EOS). Both satellites are launched on polar orbits since 1999 (Terra) and 2002 (Aqua). They overpass the equator at 10:30 a.m. and 1:30 p.m., respectively. The global coverage is provided within 1-2 days, through a nadir-looking geometry at a solar zenith angle of 45 degrees. The spatial resolution varies between 250 m and 1 km per pixel depending on the spectral band.

MODIS observes the NIR solar radiation reflected by sufficiently bright surfaces and clouds. The 36 channels cover the spectral region 0.4 - 14.4 µm and enable measurements of many other trace gases in addition to clouds and aerosols.

Five NIR channels are used for retrieving water vapour *(Gao, 2003)*. They are centred on 0.865, 0.905, 0.936, 0.94, and 1.240 µm, in which all the surface types are sufficiently bright (albedo > 0.1). The extreme channels (0.865 and 1.240 µm) have no water vapour absorption features. They are used to estimate the surface reflectance. The three other channels (0.905, 0.936, and 0.94 µm) absorb water vapour with different sensitivity. The 0.936 µm channel has the strongest absorption sensitivity. TCWV is derived by a differential absorption technique involving channels with absorption and channels without. The TCWV accuracy is claimed to be 5–10% *(Gao, 2003)*. Main uncertainties result from observations with atmospheric hazy scenes, or over dark surfaces.

The data used in this study are from the version 6 named MOD08_M3, clear column, level 3, monthly global product from the Terra Platform, gridded at 1° by 1°, freely available on: ftp://ladsweb.nascom.nasa.gov/allData/6/MOD08_M3. We used TCWV records from 2001 to 2014 for Sodankyla and Ny-Alesund, and from 2004 to 2014 for Thule to enable the comparison with GPS. TCWV data pixels were considered in similar way for both MODIS and AIRS monthly 1° by 1° gridded dataset. MODIS data coordinates at the centre of each gridded pixel, so a single pixel is considered per station (to avoid interpolation and select the nearest pixel to GNSS/IGS stations) and defined as follow:

$$(\mathrm{Lat, Lon})_{(\mathrm{Pixel})} = (\mathrm{lat, lon})_{(\mathrm{station})} + (0.5°, 0.5°), \qquad (3)$$

Where $(\mathrm{lat, lon})_{\mathrm{station}}$ are defined in Table 1 for each of the three stations.

For example Sodankyla MODIS pixel was selected as follow:

$$(\mathrm{Lat, Lon})_{(\mathrm{Soda})} = (67°, 26°)_{(\mathrm{table1})} + (0.5°, 0.5°) = (67.5°, 26.5°)$$

2.3 SCIAMACHY

Launched on board the satellite ENVISAT-1in March 2002, the Scanning Imaging Absorption spectrometer for Atmospheric CHartographY (SCIAMACHY) was designed to observe the earthshine radiance and the solar irradiance within limb and nadir alternating viewing geometry. SCIAMACHY nadir and limb observations cover the spectra from Ultra Violet (UV) to NIR (214-2380 nm) at moderate spectral resolution (0.2-1.5 nm). The observed spectra enable the measurement of many other trace gases, as well as clouds and aerosols.

SCIAMACHY can measure water vapour at various wavelengths from the VIS to the SWIR (Short-Wave Infrared). This paper uses TCWV retrieved by the Air Mass Corrected Differential Optical Absorption Spectroscopy method, shortly AMC-DOAS *(Noël et al., 2004)*, where water vapour is measured in nadir mode in the visible part of the spectrum between 688 nm and 700 nm. This method makes use of the similar slant optical depth of both O_2 and water vapour to determine an Air Mass correction Factor (AMF) which compensates for insufficient knowledge of the atmospheric and topographic background, like surface elevation and clouds.

---

[1] http://dx.doi.org/10.5067/MODIS/MOD08_M3.006

The three stations used in this study were part of the ground-based stations contributing to the SCIAMACHY validation effort *(Piters et al., 2006)* during which water vapour profiles alone were validated over Thule and Sodankyla, while TCWV was additionally validated over Ny-Alesund.

TCWV data used in this paper are from *(Noël et al., 2004)*, where all observations with AMF < 0.8 were removed, as well as those performed at solar zenith angles larger than 88°. We apply an extra screening that excludes data with SCIAMACHY indicated error > 20 % (fitting error), and swath data of spatial distance more than 50 km (actually 54 km) to the station coordinates defined by Table1.

This collocation is made by choosing data that meet the condition:

$$|\,\mathrm{Lat}_{(data)} - \mathrm{lat}_{(station)}\,| \leq 0.5° \quad \text{and} \qquad |\,\mathrm{Lon}_{(data)} - \mathrm{lon}_{(station)}\,| \leq 0.2°, \tag{4}$$

This surface is defined according to SCIAMACHY swath data footprints size which is about 30 km × 60 km.

Then, SCIAMACHY TCWV monthly means are calculated from all the matched data to the given station. Note that SCIAMACHY data solar dependency results in winter missing months that will be indicated in details later. Our study takes place from 2003 to 2011 over Sodankyla and Ny-Alesund and from 2004 to 2011 for Thule, data range is limited by SCIAMACHY and GNSS continued records availability.

2.4 AIRS

The Atmospheric Infrared System (AIRS) is carried on Aqua/EOS since May 2002. This platform has an equatorial over passing at 1:30 p.m. with a sun-synchronous orbit. AIRS was dedicated to water cycle, energy, and traces gases observations. It provides twice daily global coverage with higher vertical resolutions than all previous sensors, and comparable accuracy to radiosondes *(Tobin et al., 2006)*. AIRS is a hyper-spectral scanning infrared sounder. It measures upwelling thermal radiation emitted from the atmosphere and the surface. However, almost 30% of the AIRS radiances could be trapped below clouds (*Susskind et al., 2006)*. These possible profiles could be better retrieved using simultaneous observations from the Advanced Microwave Sounding Unit (AMSU) *(Lambrigtsen, 1999)* in a process called “cloud-clearing” *(Susskind et al., 2003)*. The observation geometry of these combined measurements or the AIRS Field of Regard (FOR) is called “AIRS golf ball”.

Humidity profiles (level 2 products) are retrieved from cloud-cleared radiances (level 1). A set of different water vapour sensitive channels are used in addition to temperature sensitive channels. Water vapour mixing ratios at certain pressure levels are retrieved using the Radiative Transfer Algorithm AIRS-RTA described by *(Strow et al., 2003).* TCWV is obtained by integrating the vertical profile of water vapour mixing ratio.

The RMSE of the AIRS water vapour profiles is estimated to 10-15% over 2-km layers in the troposphere *(Fetzer et al., 2003); (Divakarla et al., 2006).* Several studies have confirmed that both the AIRS radiances and the AIRS clear-sky forward model have an absolute accuracy of around 0.2 K for the spectral channels used in temperature and water vapour retrievals *(Fetzer et al., 2003; Strow et al., 2006).*

Previous versions of AIRS TCWV were validated against radiosondes over oceanic areas *(Fetzer et al., 2006),* and against reanalysis (EMCWF) *(Susskind et al., 2006). Gettelman et al. (2006)* showed that AIRS retrievals in polar regions are unbiased relative to in-situ radiosondes. Most results indicate a small mean bias that doesn’t exceed 10 % with no significant dependency upon cloud amount.

AIRS TCWV data *(Susskind et al., 2014)* used in this study are taken from observations in the ascending orbit mode (version 6, monthly weighted means, level 3) product, namely AIRX3STM**_006**. This data set should have high quality retrievals due to the dense orbital coverage at high latitude. Similarly to MODIS data, the 1° by 1° gridded AIRS pixels were screened. The AIRS considered TCWV pixel per station is the same as for MODIS and defined by formula (3). The comparison to GNSS is done from 2003 to 2014 for Sodankyla and Ny-Alesund and from 2004 to 2014 for Thule according to AIRS and GNSS data availability.

During this study, we additionally use the AIRS cloud fraction (CF) monthly 1° by 1° data set also in the ascending mode, namely: AIRx3STMv006 from the version 6 *(Kahn et al., 2014)* in order to study possible effects of cloud interference on the satellites observed biases. AIRS cloud fraction is used for this study as AIRS has longest overpasses (Table.1), which include (partially) both other sensors passing hours over the studied stations. AIRS effective Cloud fraction (used here) is computed as the ratio of the number of AIRS cloudy footprints to the total number of AIRS measurements per 1° by 1°, cloudy measurements are considered for CF>0.01.

3 Mean seasonal comparisons and discussion

3.1 GNSS vs MODIS

MODIS time series of monthly means TCWV are compared to monthly means of coincident overpassing (mentioned in Table 1) GNSS data over Sodankyla and Ny-Alesund for the period 2001-2014, and over Thule for 2004-2014. This difference in the data range is linked to the GNSS data availability, as GNSS dataset has some missing values at Thule during 2001-2003. The results show an excellent overall agreement with a high coefficient of correlation R > 96 % for the monthly time series (Table 2). High correlation of the monthly time series is indeed expected since the seasonal cycle is very marked at all three sites (Fig. 2). The mean biases are +0.4, +0.6, +1.7 kg m^{-2} at Ny-Alesund, Thule, and Sodankyla, respectively (Table 2). The overall positive biases indicate that MODIS generally under-estimates TCWV compared to GPS. This was previously reported over other cold regions of the world, using other versions of GNSS and MODIS data, for example, over the Tibetan plateau for both stations Gaize and Naque *(Liu et al., 2006)*. Here we can also notice a latitudinal decrease both in the absolute bias (in kg m^{-2}) and the relative bias, as well as in the root mean square errors (RMSE), which means that the TCWV retrieval is actually more accurate at higher latitudes.

The mean biases and inter-annual variability of the individual months are analysed with boxplots in Fig. 3. A seasonal variation can be seen at all three sites in the bias and in the dispersion (see the inter-quartile range in the boxplots). The largest variations are observed at Sodankyla with large positive biases between September and February, and slightly negative biases between July and August.

Dividing the year into four seasons, the statistics were also calculated and given in Table 2. At Ny-Alesund and Thule the relative bias doesn’t exceed 13% regardless of the season and the absolute biases are larger in (June-July-August) JJA and SON (September-October-November). A small wet bias is observed at Ny-Alesund during spring which was also reported for Antarctica during the transition seasons *(Thomas et al., 2011)*. The inter-annual variability is best represented for the DJF (December-January-February) and SON seasons at both high latitude sites

(Ny-Alesund and Thule) with correlations in the range 56 – 83% (all significant) but quite poorly in JJA with correlation values of 10 and 15% (not significant). The larger biases and lower correlations in JJA are linked with cloud cover (see section 4). At Sodankyla, the results are worse and more complex to interpret.

During the snow season which lasts from October to April at Sodankyla, the solar angle has a strong influence on the effective albedo, since Sodankyla is totally covered with canopy, unlike both other stations, and its forests intercept the majority of incoming solar radiation, as pointed out by *(Gryning et al., 2002)*. Additionally, Sodankyla snow samples contain higher impurity concentrations (black carbon) than measured elsewhere in Arctic Scandinavia or Greenland *(Doherty et al., 2010)*, as well as a bigger snow grain size. These two factors could also justify lower albedo *(Meinander et al., 2013a)*. The chemical exchange between polluted atmospheric layers due to winter biomass burning and snow surface opaque the lower part of the atmosphere at the instrument's wavelengths. All the previous conditions limit the MODIS retrieval capacities (Fig. 3) and could explain the smaller snow season MODIS TCWVs values at Sodankyla. During summer at Sodankyla, MODIS TCWVs were found bigger than GNSS measurements. This opposite bias can be explained by the fact that the snow coverage nearly disappeared, in addition to the tendency of increasing MODIS TCWV with increasing water vapour at sites below 3000 m *(Lu et al., 2011)*.

3.2 GNSS vs SCIAMACHY

Calculated monthly means of SCIAMACHY TCWV over Sodankyla and Ny-Alesund for 2003-2011 and over Thule for 2004-2011 were compared to means of coincident GNSS measurements. This comparison doesn't include winter pairs over Thule and Ny-Alesund because of missing SCIAMACHY measurements during polar winter. Similarly to MODIS, SCIAMACHY under-estimates TCWVs at all three sites with mean absolute biases between 0.6 and 2.4 kg m^{-2} and relative biases between 6 and 22% (Table 2). The general dry biases agrees well with previous findings by *(Van Malderen et al., 2014b)* using different versions/retrieval methods of both GNSS and SCIAMACHY data on a multi station base with a semi-hemispheric coverage. However, our study shows smaller TCWV biases confirming the improvements of recent GNSS version used and SCIAMACHY data procedures. A good overall correlation is observed between SCIAMACHY and GNSS monthly time series with R>90 % and RMSE between 24 and 27%. The monthly mean biases (Fig. 4) show also a marked seasonal variation at all three sites. The absolute biases show a similar seasonality at all stations, having their minimum during spring and maximum during summer or fall. At Ny-Alesund and Thule, the dry biases are the largest during SON and JJA, similar to MODIS but with different magnitudes. At Sodankyla the bias is around 5 kg m^{-2} in JJA, i.e. much larger and of opposite sign compared to MODIS (Table 2). The seasonal RMSE values are generally larger as well compared to MODIS at Ny-Alesund and Thule but smaller at Sodankyla where they don't exceed 30%. Inter-annual variability is generally well represented by SCIAMACHY at Ny-Alesund and Thule (R > 76% significant in all seasons except at Thule in JJA). At Sodankyla the correlations are much smaller, similarly to what we found with MODIS.

Consideration of surface albedo of complex surfaces could be also a challenge for the SCIAMACHY TCWV retrieval. The presence of snow with a nearby canopy (e.g. in Sodankyla) might result in a surface albedo significantly different from the prescribed surface albedo used in the AMC-DOAS method (e.g. 0.05 compared to 0.5) which would explain the winter biases *(Noël, 2007)*. Nevertheless, the DJF and SON absolute TCWV biases found here with SCIAMACHY are smaller than those found with MODIS. They are also smaller than those expected for SCIAMACHY in such conditions *(Noël, 2007)*. On the other hand, the JJA bias at Sodankyla is the most challenging and yet unexplained issue.

3.3 GNSS vs AIRS

The AIRS TCWV monthly product shows excellent agreement with coincident GNSS measurements at all stations. The overall correlation with GNSS is larger than 98 %, and the mean bias is smaller than 1 kg m^{-2} in absolute value (Table 2). These biases are in the same range as reported in previous studies over cold regions, e.g. *Thomas et al. (2011)* over Antarctica. However our study uses a more recent and improved version of both AIRS and GNSS data sets. Again, the monthly mean biases show a distinct seasonal variation at all three sites (Fig. 5). AIRS is found to be biased wet compared to GNSS during the colder and drier periods and biased dry during the moister months over Ny-Alesund and Thule (Fig. 5). This observed wet/dry seasonal variation of the bias is consistent with the previous validation efforts of *Rama Varma Raja et al. (2008)* and of *Van Malderen et al. (2014)*. The bias at Sodankyla follows similar seasonal variation but with an overall offset (the bias is always positive). The inter-annual variability is globally much better reproduced by AIRS than the two previous sensors as attested by the correlation coefficients > 64% (all significant except one). The correlations are higher over Ny-Alesund and Thule than Sodankyla. Compared to MODIS and SCIAMACHY, the results are noticeably better at Sodankyla (seasonal bias and RMSE < 13% and 17%, respectively). So there must be a significantly different sensitivity in the measurements to the atmospheric properties over Sodankyla. In the next section we investigate more specifically the impact of cloud cover on the TCWV retrievals from all three sensors.

4 Cloud impact on TCWV observations

MODIS and SCIAMACHY TCWV measurements are known to be sensitive to the presence of clouds, whereas the AIRS TCWV product is less impacted by clouds as it includes microwave water vapour measurements and a robust cloud clearing technique also based on microwave measurements *(Susskind et al., 2003)*. This section uses the AIRS cloud fraction product to examine the correlations between the TCWV biases found in section 3 and cloud cover. Figure 6 describes the annual cycle of cloud fraction at the three sites based on monthly mean AIRS cloud fraction product for a common period of 11 years (2004-2014). At Sodankyla, the 8-months period from May to December shows a cloud cover above 50%, with a maximum in June (> 60%) and a minimum in March (< 40 %). At Thule, the seasonal variation is even larger with 4 months < 35% (January to April) and 4 months > 50%. September has the cloudiest conditions (> 60 %) and April has the clearest (< 30%). At Ny-Alesund, cloud cover is above 44% all year long, with values > 50% during 9 months and a relative minimum (<50%) during the JJA summer months. In this section we examine the correlation coefficients between monthly TCWV biases and cloud cover with different temporal sampling. We start with the full time series of monthly means , then move on to the annual cycle (averages over all years for each of the 12 calendar months), next the inter-annual variability cycle by calendar season (DJF, MAM, JJA, SON) and finally the inter-annual variability by month.

4.1 GNSS vs MODIS

Although this study uses only clear column water vapour observations, the monthly time series of TCWV differences (GNSS-MODIS) show significant correlations with the coincident cloud fraction at Thule and Ny-Alesund, with R = 39 and 44 % respectively (all significant values are given at a significance level > 95%), unlike Sodankyla (Table 3). However, the annual cycle of TCWV biases shows significant correlation with coincident cloud fraction at Thule only (R = 69%) unlike Ny-Alesund. This different sensitivity is due to stronger annual cycle of cloud fraction at Thule in comparison with Ny-Alesund (Fig. 6). The inter-annual variability is more dominant at Ny-Alesund in spring and summer (R = 58% in JJA and MAM), with 7 significant months with R > 58 %. At Thule, the inter-annual variability is significant in three seasons (DJF, JJA, and SON) but at monthly scale, only two months are significant, November with R = 77% and December with R = 70%.

The high correlations between TCWV biases and cloud cover in JJA at both sites could explain the poor agreement found in section 3.1 (large biases 0.6 and 1.1 kg m^{-2}, and small correlations R = 10 and 15%, see Table 2) between MODIS and GNSS TCWV time series at Ny-Alesund and Thule respectively. Figure 7 gives more insight into the time series at Ny-Alesund and Thule in the most significant seasons.

Regarding Sodankyla, TCWV differences show no significant correlation with coincident cloud fraction at monthly, annual, or inter-annual variability, except during three months of the snow season (R = 71, 76 and 84 % in November, December, and March, respectively). Though cloud cover may contribute to part of the dry biases in DJF and SON reported at Sodankyla in section 3.1, the biases at this site are probably not dominated by cloud effects. We believe that the environmental features of Sodankyla which complicate the surface albedo estimation are more responsible of limiting MODIS retrieval capabilities as previously discussed in section 3.1.

4.2 GNSS vs SCIAMACHY

Like with MODIS, the monthly time series of TCWV biases are significantly correlated with cloud fraction at Ny-Alesund and Thule, with R = 26 and 60 %. However, unlike with MODIS, Sodankyla shows also a significant correlation with R = 29%.The correlations at annual scale at Thule and Ny-Alesund behave again like with MODIS. They increase at Thule (from R = 60% at monthly scale to R = 75% at annual scale) and decrease at Ny-Alesund (from R = 26% to -19%), while at Sodankyla the annual variations are strongly correlated at R = 75 %.

Our results show thus that SCIAMACHY’s TCWV retrieval is more sensitive to cloud cover than the MODIS one. This is consistent with the findings of Palm et al., (2010) who concluded that cloudy conditions introduce a severe bias at Ny-Alesund, even if the SCIAMACHY measurement passes the cloud screening filter.

As found with MODIS (section 4.1), TCWV biases and cloud cover are strongly correlated at the inter-annual scale in JJA at both Ny-Alesund and Thule with R = 72 % (Table 3). This sensitivity is due to the strong inter-annual variability at both sites in JJA (Fig. 8). At Sodankyla, the inter-annual variability in TCWV biases and cloud fraction are not significantly correlated except in May with R = -77% (Table. 3). This anti-correlation is not explained yet.

4.3 GNSS vs AIRS

The results with AIRS are quite different compared to SCIAMACHY and MODIS. Whereas monthly time series of TCWV biases show significant positive correlation with cloud fraction at Thule (R = 31%), the correlation is negative at Ny-Alesund (R = -42%). The negative correlation at Ny-Alesund is explained by the pronounced but opposite annual variations of the TCWV biases (Fig. 5) and the cloud cover (Fig. 6) at this site, with an annual correlation of R = -94% (Table. 3). The inter-annual variability of TCWV biases and cloud cover are generally not significant, except for DJF at Ny-Alesund (R = -63%) and a few individual months (Table 3). Figure 9 shows the DJF time series at Thule and Ny-Alesund. No summer sensitivity to cloud fraction is found as for MODIS and SCIAMACHY. At Sodankyla no significant correlations are found for the monthly means and the annual cycle. At inter-annual scale, only March shows a significant positive correlation (R = 61 %), similar to MODIS.

Overall, Ny-Alesund TCWV AIRS biases seasonality is almost linear with negative slope with cloud fraction. Moreover, the dominated wet biases in winter (AIRS measurements are bigger than those of GNSS unlike SCIAMACHY and MODIS, see Table 2) are found to be sensitive to cloud fraction (Table. 3). Results don’t show summer sensitivity to cloud fraction as found for MODIS and SCIAMACHY. Most correlations found are sparse temporally and don’t show clear features. This might be due to the fact that AIRS TCWV biases are smaller in magnitude (Table. 2) and show a different seasonality compared to MODIS and SCIAMACHY.

5 Conclusions

This paper found a very good agreement between satellite measurements and coincident GPS, with however some regional features of biases. Nearly all satellites TCWVs show dry biases compared to GPS, all year-long, with some exceptions as with AIRS wet bias in winter and fall. We generally see better agreement (higher correlation, smaller bias and RMSE) between GNSS and AIRS TCWV time series than between GNSS and MODIS or SCIAMACHY. The absolute biases don’t exceed 1 kg m^{-2} with AIRS, except in summer at Sodankyla where the bias reaches 1.5 kg m^{-2}. At Sodankyla, the agreement between GNSS and satellite retrievals is lower for all three satellite measurements. We don’t suspect the GNSS data as they passed a selective quality control and outlier detection procedure. Instead, we hypothesize that satellite retrievals are impact by local effects (cloud cover and canopy).

For MODIS, the inter-annual agreement is getting better with latitude over all seasons except summer. During summer, the inter-annual variability is actually getting worse at higher latitudes sites. These increase summer biases are found to be sensitive to clouds cover. Additionally, MODIS dry biases during some snowy months at Sodankyla are also correlated with cloud fraction. However, the inaccurate estimation of the surface albedo over a complex mixed surface (snow and nearby canopies) also limits the MODIS retrieval capabilities at Sodankyla.

Summer SCIAMACHY TCWV biases are found correlated to clouds cover at the higher latitudes sites (Thule and Ny-Alesund), in similar way as MODIS ones, but unlike AIRS. However, SCIAMACHY seems to be more sensitive to cloud fraction than MODIS as the annual cycle of TCWV bias for SCIAMACHY is well correlated with the annual variations of cloud fraction at Thule and Sodankyla, while MODIS annual cycle of biases show this sensitivity to clouds only at Thule. AIRS time series of TCWV differences to GNSS show a limited link with cloud fraction compared to MODIS and SCIAMACHY with no clear features. Results reveal anti-correlated monthly differences with cloud fraction at Ny-Alesund, probably due to opposite correlation with clouds in winter.

Overall, our results suggest a probable link between satellites TCWV biases to GNSS and cloud cover fraction, with contrasted regional and seasonal features. This sensitivity is stronger at the higher latitudes. We suggest that more robust information on clouds is included in the satellite data processing procedures in order to reduce the TCWV biases in the Arctic, and then improve space-borne instrumental uncertainties. This publication recommends the use of GNSS/TCWV in the calibration of similar satellite measurements.

Acknowledgements. This work was developed in the framework of the VEGA project and supported by the French program LEFE/INSU. This work is a contribution to the European COST Action ES1206 GNSS4SWEC (GNSS for Severe Weather and Climate monitoring; http://www.cost.eu/COST_Actions/essem/ES1206) aiming at the development of the global GNSS network for atmospheric research and climate change monitoring. The authors would like to thank Jan Dousa, GOP, Czech Republic, for providing the reprocessed GPS ZTD data, and the staff from the Climserv data centre at IPSL for providing the ERA-Interim data

References

Bevis, M., Businger, S., Herring, T. A., Rocken, C., Anthes, R. A. and Ware, R. H.: GPS meteorology: Remote sensing of atmospheric water vapor using the Global Positioning System, J. Geophys. Res. Atmos., 97(D14), 15787–15801, 1992a.

Bevis, M., Businger, S., Herring, T. ~A., Rocken, C., Anthes, R. ~A. and Ware, R. ~H.: GPS Meteorology: Remote Sensing of Atmospheric Water Vapor Using the Global Positioning System, \Jgr, 97(92), 15787–15801, 1992b.

Bock, O.: GNSS: geodesie, meteorologie et climat. Ocean, Atmosphere., 2012.

Bock, O. and Nuret, M.: Verification of NWP Model Analyses and Radiosonde Humidity Data with GPS Precipitable Water Vapor Estimates during AMMA, Weather Forecast., 24(4), 1085–1101, doi:10.1175/2009WAF2222239.1, 2009.

Bock, O., Bouin, M. N., Walpersdorf, A., Lafore, J. P., Janicot, S., Guichard, F. and Agusti-Panareda, A.: Comparison of ground-based GPS precipitable water vapour to independent observations and NWP model reanalyses over Africa, Q. J. R. Meteorol. Soc., 133(629 B), 2011–2027, 2007.

Bock, O., Willis, P., Wang, J. and Mears, C.: A high-quality, homogenized, global, long-term (1993-2008) DORIS precipitable water data set for climate monitoring and model verification, J. Geophys. Res. Atmos., 119(12), 7209–7230, doi:10.1002/2013JD021124, 2014.

Chahine, M. T.: The hydrological cycle and its influence on climate, Nature, 359, 6394, 359(6394), 373–380, doi:10.1038/359373a0, 1992.

Chen, Y., Miller, J. R., Francis, J. a and Russell, G. L.: Projected regime shift in Arctic cloud and water vapor feedbacks, Environ. Res. Lett., 6, 44007, doi:10.1088/1748-9326/6/4/044007, 2011.

Davis, J. L., Herring, T. A., Shapiro, I. I., Rogers, A. E. E. and Elgered, G.: Geodesy by radio interferometry: Effects of atmospheric modeling errors on estimates of baseline length, Radio Sci., 20(6), 1593–1607, 1985.

Dee, D. P., Uppala, S. M., Simmons, A. J., Berrisford, P., Poli, P., Kobayashi, S., Andrae, U., Balmaseda, M. A., Balsamo, G., Bauer, P. and others: The ERA-Interim reanalysis: Configuration and performance of the data assimilation system, Q. J. R. Meteorol. Soc., 137(656), 553–597, 2011.

Divakarla, M. G., Barnet, C. D., Goldberg, M. D., McMillin, L. M., Maddy, E., Wolf, W., Zhou, L. and Liu, X.: Validation of Atmospheric Infrared Sounder temperature and water vapor retrievals with matched radiosonde measurements and forecasts, J. Geophys. Res. Atmos., 111(9), 1–20, doi:10.1029/2005JD006116, 2006.

Doherty, S. J., Warren, S. G., Grenfell, T. C., Clarke, A. D. and Brandt, R. E.: Light-absorbing impurities in Arctic snow, Atmos. Chem. Phys., 10(23), 11647–11680, doi:10.5194/acp-10-11647-2010, 2010.

Dousa, J. and Vaclavovic, P. .: Tropospheric products of the 2nd European reprocessing (1996–2014), Atmos. Meas. Tech. Discuss., doi:doi:10.5194/amt-2017-11, 2017.

Fetzer, E., Mcmillin, L. M., Tobin, D., Aumann, H. H., Gunson, M. R., Mcmillan, W. W., Hagan, D. E., Hofstadter, M. D., Yoe, J., Whiteman, D. N., Barnes, J. E., Bennartz, R., Vömel, H., Walden, V., Newchurch, M., Minnett, P. J., Atlas, R., Schmidlin, F., Olsen, E. T., Goldberg, M. D., Zhou, S., Ding, H., Smith, W. L. and Revercomb, H.: AIRS / AMSU / HSB Validation, , 41(2), 418–431, 2003.

Fetzer, E. J., Lambrigtsen, B. H., Eldering, A., Aumann, H. H. and Chahine, M. T.: Biases in total precipitable water vapor climatologies from Atmospheric Infrared Sounder and Advanced Microwave Scanning Radiometer, J. Geophys. Res. Atmos., 111(9), 2006.

Francis, J. and Hunter, E.: Changes in the fabric of the Arctic’s greenhouse blanket, Environ. Res. Lett., 2(4), 45011, doi:10.1088/1748-9326/2/4/045011, 2007.

Gaffen, D. J.: Temporal inhomogeneities in radiosonde temperature records, J. Geophys. Res. Ser., 99, 3667, 1994.

Gao, B.-C.: Water vapor retrievals using Moderate Resolution Imaging Spectroradiometer (MODIS) near-infrared channels, J. Geophys. Res., 108(D13), 1–10, doi:10.1029/2002JD003023, 2003.

Gao, B.-C. and Kaufman, Y. J.: Water vapor retrievals using Moderate Resolution Imaging Spectroradiometer (MODIS) near-infrared channels, J. Geophys. Res. Atmos., 108(D13), n/a-n/a, doi:10.1029/2002JD003023, 2003.

Gettelman, A., Fetzer, E. J., Eldering, A. and Irion, F. W.: The global distribution of supersaturation in the upper troposphere from the Atmospheric Infrared Sounder, J. Clim., 19(23), 6089–6103, doi:10.1175/JCLI3955.1, 2006.

Ghatak, D. and Miller, J.: Implications for Arctic amplification of changes in the strength of the water vapor feedback, J. Geophys. Res. Atmos., 118(14), 7569–7578, doi:10.1002/jgrd.50578, 2013.

Gryning, S., Halldin, S. and Lindroth, A.: Area averaging of land surface – atmosphere fluxes in NOPEX : challenges , results and perspectives, , (December), 379–387, 2002.

Guerova, G., Brockmann, E., Schubiger, F., Morland, J. and Mätzler, C.: An Integrated Assessment of Measured and Modeled Integrated Water Vapor in Switzerland for the Period 2001-03, J. Appl. Meteorol., 44(7), 1033–1044, doi:10.1175/JAM2255.1, 2005.

Guerova, G., Jones, J., Dou, J., Dick, G., Pottiaux, E., Bock, O., Pacione, R., Elgered, G., Vedel, H. and Bender, M.: Review of the state-of-the-art and future prospects of the ground-based GNSS meteorology in Europe, , (June), 1–34, doi:10.5194/amt-2016-125, 2016.

Hanesiak, J., Melsness, M. and Raddatz, R.: Observed and modeled growing-season diurnal precipitable water vapor in south-central Canada, J. Appl. Meteorol. Climatol., 49(11), 2301–2314, doi:10.1175/2010JAMC2443.1, 2010.

Held, I. M. and Soden, B. J.: Water Vapor Feedback and Global Warming, Annu. Rev. Energy Environ., 25(1), 441–475, doi:10.1146/annurev.energy.25.1.441, 2000.

Jones, P. D., Trenberth, K. E., Ambenje, P., Bojariu, R., Easterling, D., Klein, T., Parker, D., Renwick, J., Rusticucci, M., Soden, B. and others: Observations: surface and atmospheric climate change, Clim. Chang. 2007 Phys. Sci. basis. Contrib. Work. Gr. I to Fourth Assess. Rep. Intergov. Panel Clim. Chang., 235–336, 2007.

Kahn, B. H., Irion, F. W., Dang, V. T., Manning, E. M., Nasiri, S. L., Naud, C. M., Blaisdell, J. M., Schreier, M. M., Yue, Q., Bowman, K. W., Fetzer, E. J., Hulley, G. C., Liou, K. N., Lubin, D., Ou, S. C., Susskind, J., Takano, Y., Tian, B. and Worden, J. R.: The atmospheric infrared sounder version 6 cloud products, Atmos. Chem. Phys., 14(1), 399–426, doi:10.5194/acp-14-399-2014, 2014.

Kiehl, J. T. and Trenberth, K. E.: Earth’s Annual Global Mean Energy Budget, Bull. Am. Meteorol. Soc., doi:10.1175/1520-0477(1997)078<0197:EAGMEB>2.0.CO;2, 1997.

Lambrigtsen, B. H.: AIRS Project Algorithm Theoretical Basis Document Level l b Part 3: Microwave Instruments, 1999.

Liu, J., Liang, H., Sun, Z. and Zhou, X.: Validation of the Moderate-Resolution Imaging Spectroradiometer precipitable water vapor product using measurements from GPS on the Tibetan Plateau, J. Geophys. Res. Atmos., 111(14), 1–5, doi:10.1029/2005JD007028, 2006.

Lu, N., Qin, J., Yang, K., Gao, Y., Xu, X. and Koike, T.: On the use of GPS measurements for Moderate Resolution Imaging Spectrometer precipitable water vapor evaluation over southern Tibet, J. Geophys. Res. Atmos., 116(23), 1–7, doi:10.1029/2011JD016160, 2011.

Van Malderen, R., Brenot, H., Pottiaux, E., Beirle, S., Hermans, C., De Mazi??re, M., Wagner, T., De Backer, H. and Bruyninx, C.: A multi-site intercomparison of integrated water vapour observations for climate change analysis, Atmos. Meas. Tech., 7(8), 2487–2512, doi:10.5194/amt-7-2487-2014, 2014a.

Van Malderen, R., Brenot, H., Pottiaux, E., Beirle, S., Hermans, C., De Mazière, M., Wagner, T., De Backer, H. and Bruyninx, C.: A multi - site intercomparison of integrated water vapour observations for climate change analysis, Atmos . Meas . Tech, 7, 2487–2512, doi:10.5194/amtd-7-1075-2014, 2014b.

Meinander, O., Kazadzis, S., Arola, A., Riihelä, A., Räisänen, P., Kivi, R., Kontu, A., Kouznetsov, R., Sofiev, M., Svensson, J., Suokanerva, H., Aaltonen, V., Manninen, T., Roujean, J.-L. and Hautecoeur, O.: Geoscientific Instrumentation Methods and Data Systems Spectral albedo of seasonal snow during intensive melt period at Sodankylä, beyond the Arctic Circle, Atmos. Chem. Phys, 13, 3793–3810, doi:10.5194/acp-13-3793-2013, 2013a.

Miller, J. R., Chen, Y., Russell, G. L. and Francis, J. A.: Future regime shift in feedbacks during Arctic winter, Geophys. Res. Lett., 34(23), 7–10, doi:10.1029/2007GL031826, 2007.

Noël, S.: Product Specification Document for SCIAMACHY water vapour column swath data derived using the AMC-DOAS method., 2007.

Noël, S., Buchwitz, M. and Burrows, J. P.: First retrieval of global water vapour column amounts from SCIAMACHY measurements, Atmos. Chem. Phys., 4(1), 111–125, doi:10.5194/acp-4-111-2004, 2004.

Palm, M., Melsheimer, C., Noel, S., Heise, S., Notholt, J., Burrows, J. and Schrems, O.: Integrated water vapor above Ny Alesund, Spitsbergen: a multi-sensor intercomparison, Atmos. Chem. Phys., 10(3), 1215–1226, doi:10.5194/acp-10-1215-2010, 2010.

Piters, A. J. M., Bramstedt, K., Lambert, J.-C. and Kirchhoff, B.: Overview of SCIAMACHY validation: 2002-2004, Atmos. Chem. Phys., 6(1), 127–148, doi:10.5194/acpd-5-7769-2005, 2006.

Rama Varma Raja, M. K., Gutman, S. I., Yoe, J. G., McMillin, L. M. and Zhao, J.: The validation of AIRS retrievals of integrated precipitable water vapor using measurements from a network of ground-based GPS receivers over contiguous United States, J. Atmos. Ocean. Technol., 25(3), 416–428, doi:10.1175/2007JTECHA889.1, 2008.

Ramanathan, V. and Inamdar, A.: The radiative forcing due to clouds and water vapor, Front. Clim. Model., 119–151, doi:10.1017/CBO9780511535857.006, 2006.

Rangwala, I., Miller, J. R. and Xu, M.: Warming in the Tibetan Plateau: Possible influences of the changes in surface water vapor, Geophys. Res. Lett., 36(6), 1–6, doi:10.1029/2009GL037245, 2009.

Ruckstuhl, C., Philipona, R., Morland, J. and Ohmura, A.: Observed relationship between surface specific humidity, integrated water vapor, and longwave downward radiation at different altitudes, J. Geophys. Res., 112(D3), 1–7, doi:10.1029/2006JD007850, 2007.

Schneider, E. K., Kirtman, B. P. and Lindzen, R. S.: Tropospheric Water Vapor and Climate Sensitivity, J. Atmos. Sci., 56, 1649–1658, doi:10.1175/1520-0469(1999)056<1649:TWVACS>2.0.CO;2, 1999.

Schneider, T., O’Gorman, P. a. and Levine, X.: Water vapor and the dynamics of climate changes, Rev. Geophys., (48), 1–22, doi:10.1029/2009RG000302.1.INTRODUCTION, 2010.

Screen, J. a and Simmonds, I.: The central role of diminishing sea ice in recent Arctic temperature amplification., Nature, 464(7293), 1334–1337, doi:10.1038/nature09051, 2010.

Serreze, M. C., Barrett, A. P., Slater, A. G., Woodgate, R. A., Aagaard, K., Lammers, R. B., Steele, M., Moritz, R., Meredith, M. and Lee, C. M.: The large-scale freshwater cycle of the Arctic, J. Geophys. Res. Ocean., doi:10.1029/2005JC003424, 2006.

Sherwood, S. C., Roca, R., Weckwerth, T. M. and Andronova, N. G.: Tropospheric Water Vapor , Convection , and Climate, , 48(2009), 1–29, doi:10.1029/2009RG000301.1.INTRODUCTION, 2010.

Strow, L. L., Hannon, S. E., De Souza-Machado, S., Motteler, H. E. and Tobin, D.: An Overview of the AIRS Radiative Transfer Model, IEEE Trans. Geosci. Remote Sens., 41(2), doi:10.1109/TGRS.2002.808244, 2003.

Strow, L. L., Hannon, S. E., De-Souza Machado, S., Motteler, H. E. and Tobin, D. C.: Validation of the Atmospheric Infrared Sounder radiative transfer algorithm, J. Geophys. Res. Atmos., 111(D9), 2006.

Susskind, J., Barnet, C. D. and Blaisdell, J. M.: Retrieval of Atmospheric and Surface Parameters From AIRS / AMSU / HSB Data in the Presence of Clouds, , 41(2), 390–409, 2003.

Susskind, J., Barnet, C. D., Blaisdell, J. M., Iredell, L., Keita, F., Kouvaris, L., Molnar, G. and Chahine, M. T.: Accuracy of Geophysical Parameters Derived from AIRS/AMSU as a Function of Fractional Cloud Cover, J. Geophys. Res., 111(D9), D09S17, 2006.

Susskind, J., Blaisdell, J. M. and Iredell, L.: Improved methodology for surface and atmospheric soundings, error estimates, and quality control procedures: the atmospheric infrared sounder science team version-6 retrieval algorithm, J. Appl. Remote Sens., 8(1), 84994, doi:10.1117/1.JRS.8.084994, 2014.

Thomas, I. D., King, M. A., Clarke, P. J. and Penna, N. T.: Precipitable water vapor estimates from homogeneously reprocessed GPS data: An intertechnique comparison in Antarctica, J. Geophys. Res. Atmos., doi:10.1029/2010JD013889, 2011.

Tobin, D. C., Revercomb, H. E., Knuteson, R. O., Lesht, B. M., Strow, L. L., Hannon, S. E., Feltz, W. F., Moy, L. A., Fetzer, E. J. and Cress, T. S.: Atmospheric Radiation Measurement site atmospheric state best estimates for

Atmospheric Infrared Sounder temperature and water vapor retrieval validation, J. Geophys. Res. Atmos., 111(9), 1–18, doi:10.1029/2005JD006103, 2006.

Trenberth, K. E. and Stepaniak, D. P.: Covariability of Components of Poleward Atmospheric Energy Transports on Seasonal and Interannual Timescales, J. Clim., 16(22), 3691–3705, doi:10.1175/1520-0442(2003)016<3691:COCOPA>2.0.CO;2, 2003.

Trenberth, K. E., Fasullo, J. and Smith, L.: Trends and variability in column-integrated atmospheric water vapor, Clim. Dyn., 24(7–8), 741–758, 2005.

Trenberth, K. E., Smith, L., Qian, T., Dai, A. and Fasullo, J.: Estimates of the Global Water Budget and Its Annual Cycle Using Observational and Model Data, J. Hydrometeorol., 8(4), 758–769, doi:10.1175/JHM600.1, 2007.

Wang, J.: Performance of operational radiosonde humidity sensors in direct comparison with a chilled mirror dew-point hygrometer and its climate implication, Geophys. Res. Lett., 30(16), 10–13, doi:10.1029/2003GL016985, 2003.

Wang, J. and Zhang, L.: Systematic errors in global radiosonde precipitable water data from comparisons with groud-based GPS measurements, J. Clim., 21(10), 2218–2238, doi:10.1175/2007JCLI1944.1, 2008.

Wang, J. and Zhang, L.: Climate applications of a global, 2-hourly atmospheric precipitable water dataset derived from IGS tropospheric products, J. Geod., 83(3–4), 209–217, doi:10.1007/s00190-008-0238-5, 2009.

Winton, M.: Amplified Arctic climate change: What does surface albedo feedback have to do with it?, Geophys. Res. Lett., 33(3), 1–4, doi:10.1029/2005GL025244, 2006.

Table 1: Over passing hours of each sensor in universal time (UT) at three GNSS sites

Station\instrument	MODIS (UT)	SCIAMACHY (UT)	AIRS(UT)
Sodankyla (67° N,26° E)	08 – 12 & 17 – 21	08 – 11 & 17 – 20	23 – 03 & 09 – 12
Thule (76° N,69° W)	15 – 04	16 – 20 & 22 – 02	06 – 19
Ny-Alesund (78° N,12° E)	09 – 22	10 – 20	23 – 13

Table 2 : Bias, RMSE and linear correlation coefficient between MODIS NIR, SCIAMACHY VIS, AIRS IR clear column TCWV retrievals and GNSS TCWV estimates, at Ny-Alesund (78° N, 12° E), Thule (76° N, 69° W), and Sodankyla (67° N, 26° E). Correlations with significance level > 95% are in bold.

	Station (Period)	Season	N of pairs	Bias (kg/m^2)	Bias (%)	RMSE (%)	R (%)
GNSS vs. MODIS	Ny-Alesund (2001-2014)	Monthly	168	0.4	3	18	**96**
		DJF	13	0.4	9	14	**77**
		MAM	14	0.0	-0.6	14	58
		JJA	14	0.6	4	7	10
		SON	14	0.8	12	13	**56**
	Thule (2004-2014)	Monthly	132	0.6	10	16	**98**
		DJF	10	0.3	13	17	**83**
		MAM	11	0.4	10	13	**71**
		JJA	11	1.1	10	14	15
		SON	11	0.6	13	14	**83**
	Sodankyla (2001-2014)	Monthly	166	1.7	24	33	**96**
		DJF	13	2.8	47	48	30
		MAM	14	1.5	18	19	**74**
		JJA	14	-1.1	-6	9	41
		SON	14	3.5	32	32	**76**
GNSS vs. SCIAMACHY	Ny-Alesund (2003-2011)	Monthly	81	1.5	22	27	**97**
		DJF	-	-	-	-	-
		MAM	9	1.1	22	23	**81**
		JJA	9	1.7	14	14	**76**
		SON	9	1.9	24	25	**76**
	Thule (2004-2011)	Monthly	72	0.6	6	24	**96**
		DJF	-	-	-	-	-
		MAM	8	-0.2	-5	9	**88**
		JJA	8	1.1	10	11	69
		SON	8	1.4	25	26	**90**
	Sodankyla (2003-2011)	Monthly	98	2.4	19	25	**90**
		DJF	8	1.1	21	27	26
		MAM	9	1.4	17	18	**71**
		JJA	9	4.9	27	29	19
		SON	9	1.8	16	18	48
GNSS vs. AIRS	Ny-Alesund (2003-2014)	Monthly	144	-0.1	-8	19	**98**
		DJF	11	-0.8	-22	26	**83**
		MAM	12	-0	-2	4	**97**
		JJA	12	1	9	9	**94**
		SON	12	-0.6	-8	9	**96**
	Thule (2004-2014)	Monthly	132	-0.3	-18	31	**99**
		DJF	11	-0.8	-41	44	**97**
		MAM	11	-0.3	-9	14	**85**
		JJA	11	0.5	4	5	**82**
		SON	11	-0.5	-11	12	**92**
	Sodankyla (2003-2014)	Monthly	142	1	9	14	**98**
		DJF	11	0.8	13	17	50
		MAM	12	0.7	9	9	**90**
		JJA	12	1.5	8	10	**64**
		SON	12	1	8	11	**58**

Table 3: Correlation coefficients (%) between TCWV biases and coincident cloud cover at Sodankyla (SODA) (67° N, 26° E), Thule (THUL) (76° N, 69° W), and Ny-Alesund (NYAL) (78° N, 12° E) for all months, annual cycle, and inter-annual variability (by season and by month). Correlations with significance level > 95% are in bold.

	MODIS			SCIAMACHY			AIRS		
	SODA	THUL	NYAL	SODA	THUL	NYAL	SODA	THUL	NYAL
Monthly	-3	**39**	**44**	**29**	**60**	**26**	12	**31**	**-42**
An-cycle	-38	**68**	6	**75**	**75**	-19	36	42	**-94**
DJF	43	**69**	53	-49	-	-	-18	44	**-63**
MAM	46	15	**58**	-37	18	5	4	9	17
JJA	53	**68**	**58**	27	**72**	**72**	36	49	56
SON	14	**69**	53	-42	-3	36	-24	0	18
Jan	18	48	**58**	30	-	-	-9	18	-47
Feb	51	52	44	-32	47	57	25	20	7
Mar	**84**	17	**78**	31	32	42	**61**	21	32
Apr	24	-10	42	-31	-26	23	5	-18	13
May	43	52	49	**-77**	23	30	45	**65**	34
Jun	44	51	0	7	-15	34	-13	44	**-63**
Jul	37	57	**81**	29	**75**	**80**	27	29	52
Aug	22	-32	**81**	-33	**73**	60	-10	16	-14
Sep	7	2	**58**	-40	7	37	-6	**-68**	33
Oct	-12	-8	10	-29	55	35	-24	10	-27
Nov	**71**	**77**	**65**	-27	-	-	-47	16	-27
Dec	**76**	**70**	**73**	-	-	-	11	34	-9

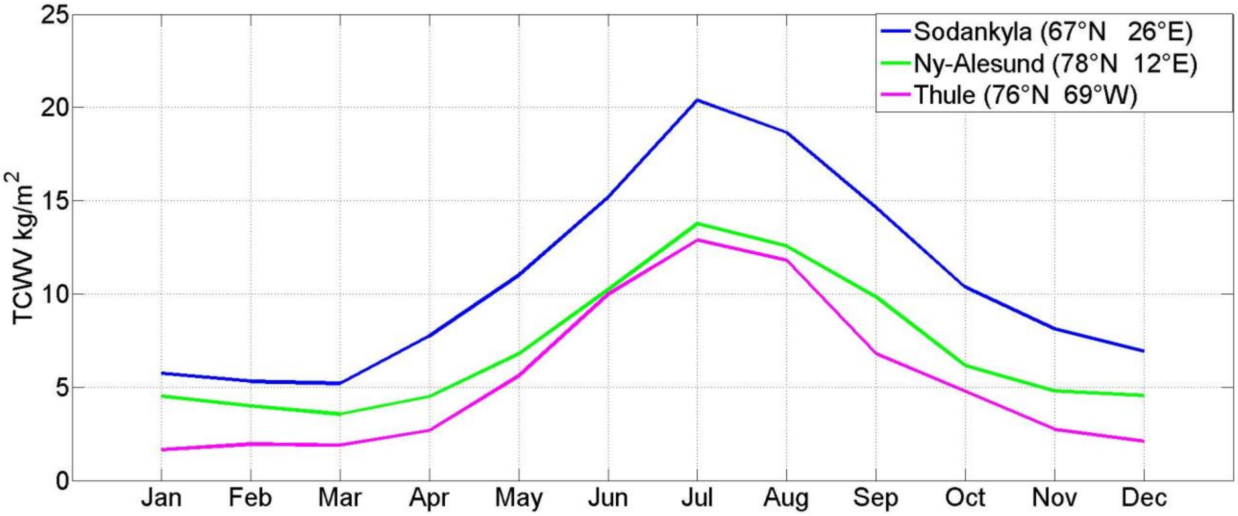

Figure 1 : Annual cycle of TCWV from GNSS for the period 2004 to 2014 (in kg m^{-2}).

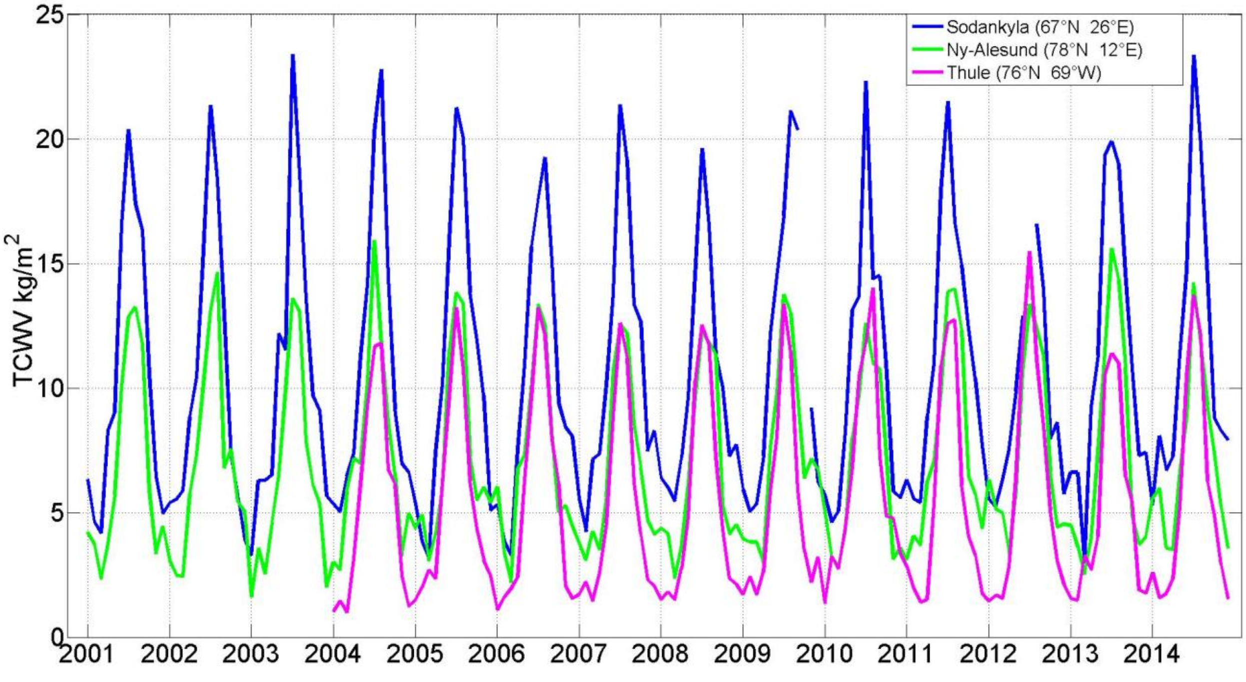

Figure 2: Monthly time series of TCWV from GNSS over the full period of observation at each site (in kg m^{-2}).

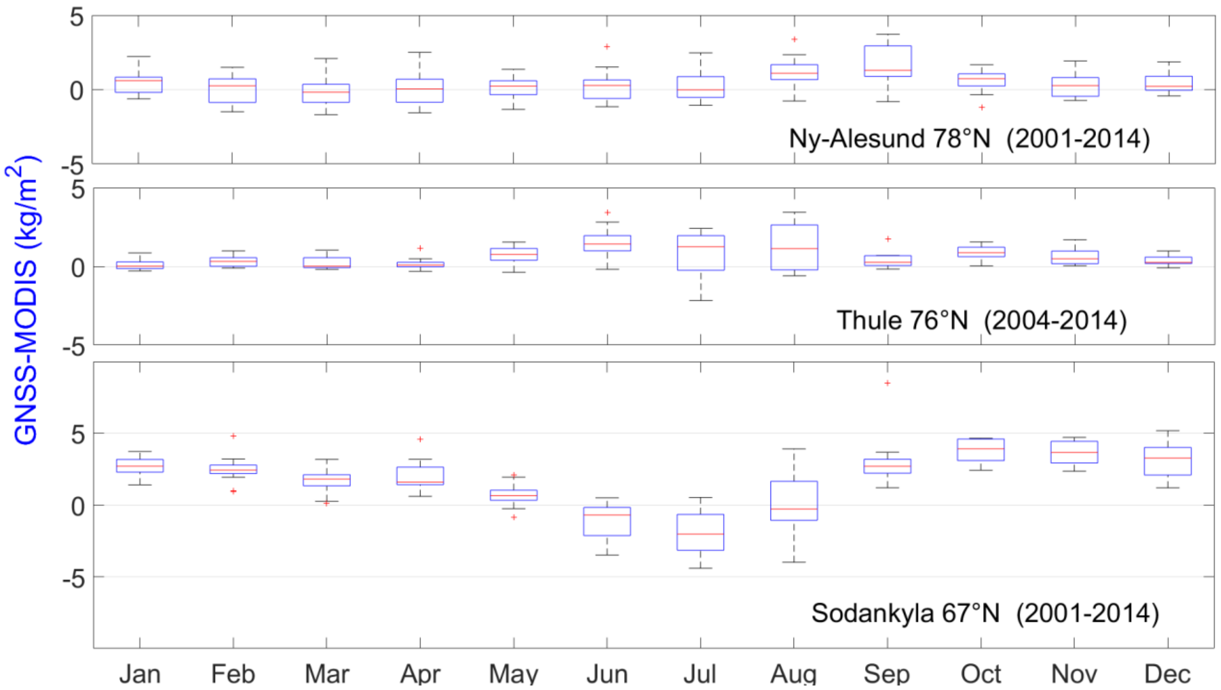

Figure 3: Box plot of the TCWV differences (GNSS - MODIS) for (2001-2014) at Sodankyla (67° N, 26° E) and Ny-Alesund (78° N, 12° E), and at Thule (76° N, 69° W) for (2004-2014) in kg m^{-2}. The central red mark indicates the median absolute TCWV difference of the month for the whole period; blue boxes indicate the 25th and 75th percentiles, respectively; black bars (whiskers) extend to ± 1.5 times the inter-quartile range from the median; Outliers are displayed using the '+' symbol.

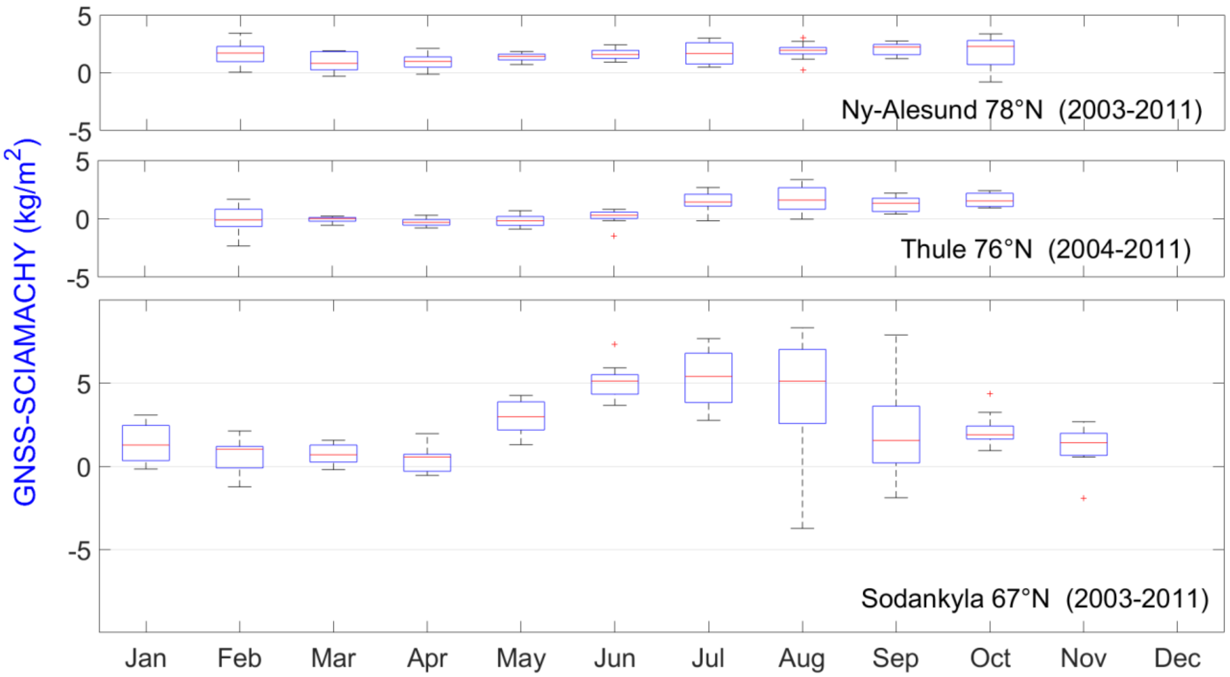

Figure 4: Box plot of the difference (GNSS - SCIAMACHY) at Sodankyla (67° N, 26° E) and Ny-Alesund (78° N, 12° E) for (2003-2011), and at Thule (76° N, 69° W) for (2004-2011) in kg m^{-2}. The boxplot indications are same as Fig. 3.

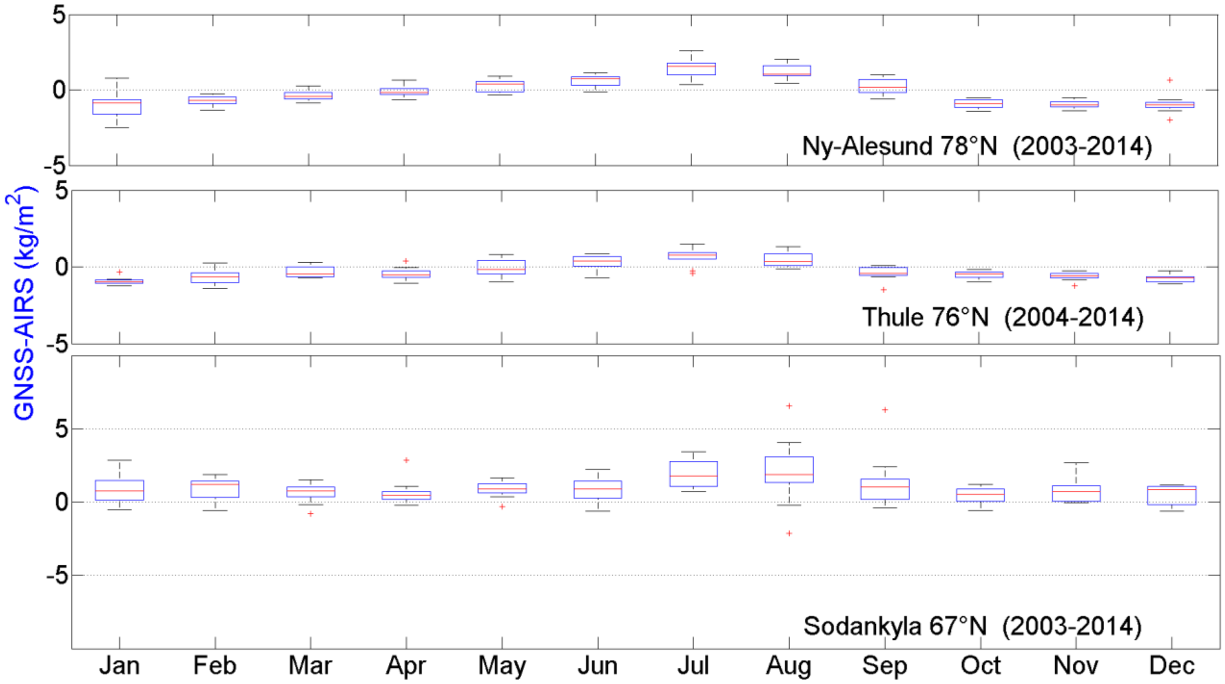

Figure 5 : Box plot of the difference (GNSS - AIRS) for (2003-2014) at Sodankyla (67° N, 26° E) and Ny-Alesund (78° N, 12° E), and for (2004-2014) at Thule (76° N, 69° W) in kg m^{-2}. The boxplot indications are same as Fig. 3.

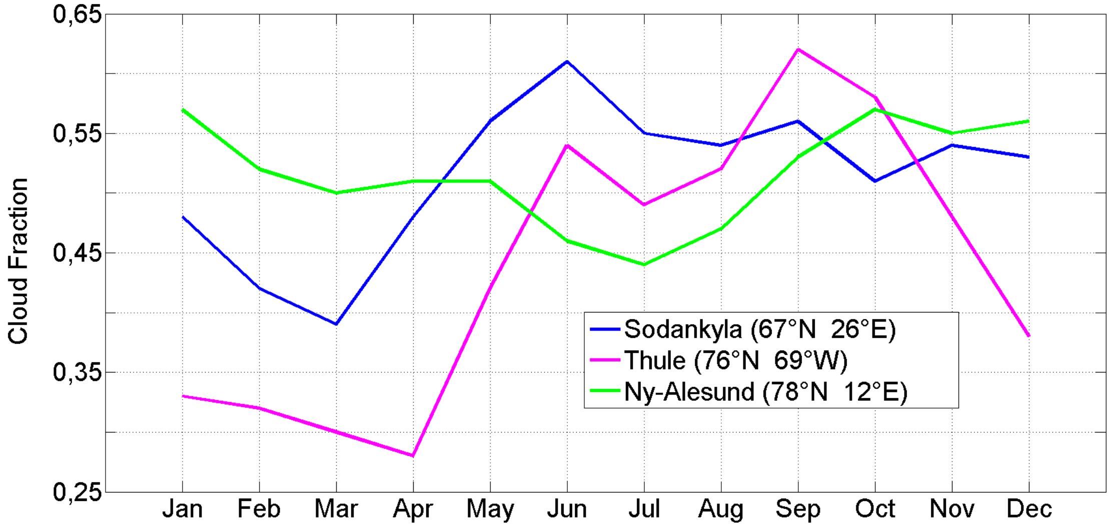

Figure 6: Annual cycle of AIRS cloud fraction for 2004-2014.

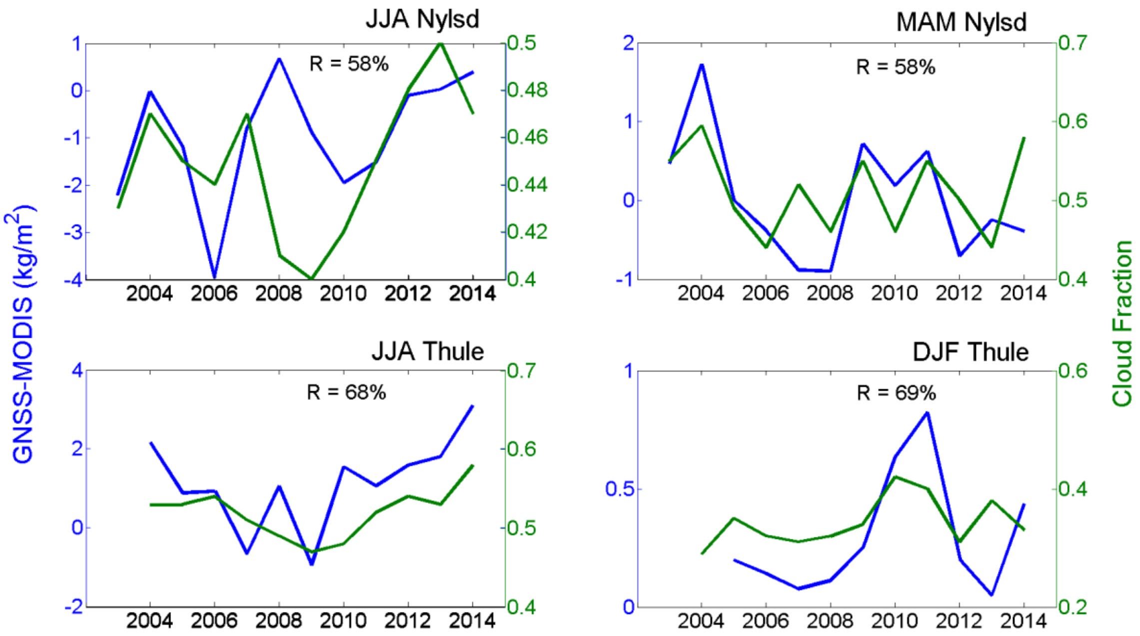

Figure 7: GNSS – MODIS TCWV differences (kg m^{-2}) and cloud fraction at Ny-Alesund (78° N, 12° E) on JJA, and MAM; and at Thule (76° N, 69° W) on JJA, and DJF for (2003-2014).

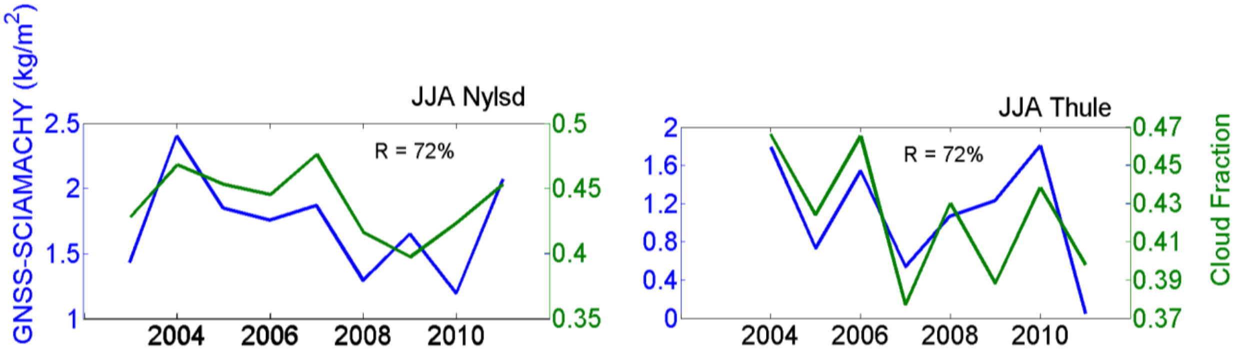

Figure 8: GNSS – SCIAMACHY TCWV differences (kg m^{-2}) and cloud fraction on JJA at Ny-Alesund (78° N, 12° E) and Thule (76° N, 69° W) for (2003-2011).

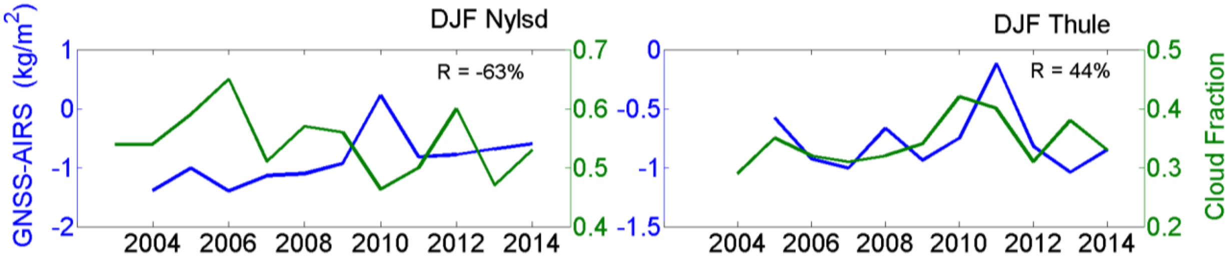

Figure 9: GNSS – AIRS TCWV differences (kg m^{-2}) and cloud fraction on DJF at Ny-Alesund (78° N, 69° W) and Thule (76°N, 69°W) for (2003-2014).